

Air lasing: Phenomena and mechanisms

Helong Li(李贺龙), Danwen Yao(姚丹雯), Siqi Wang(王思琪), Yao Fu(付尧), Huailiang Xu(徐淮良)
Citation: Chin. Phys. B . 2019, 28(11): 114204 . **doi:** 10.1088/1674-1056/ab47f5
Journal homepage: http://cpb.iphy.ac.cn; http://iopscience.iop.org/cpb

What follows is a list of articles you may be interested in

Resolving multi-orbital effects on high harmonic generation from aligned N_2 molecules in linearly and elliptically polarized intense laser fields

Hong-Jing Liang(梁红静), Xin Fan(范鑫), Shuang Feng(冯爽), Li-Yu Shan(单立宇), Qing-Hua Gao(高庆华), Bo Yan(闫博), Ri Ma(马日), Hai-Feng Xu(徐海峰), Da-Jun Ding(丁大军)
Chin. Phys. B . 2019, 28(9): 094211 . **doi:** 10.1088/1674-1056/ab3440

Attosecond transient absorption spectroscopy: Comparative study based on three-level modeling

Zeng-Qiang Yang(杨增强), Di-Fa Ye(叶地发), Li-Bin Fu(傅立斌)
Chin. Phys. B . 2018, 27(1): 013301 . **doi:** 10.1088/1674-1056/27/1/013301

Frequency dependence of quantum path interference in non-collinear high-order harmonic generation

Shi-Yang Zhong(钟诗阳), Xin-Kui He(贺新奎), Hao Teng(滕浩), Peng Ye(叶蓬), Li-Feng Wang(汪礼锋), Peng He(何鹏), Zhi-Yi Wei(魏志义)
Chin. Phys. B . 2016, 25(2): 023301 . **doi:** 10.1088/1674-1056/25/2/023301

Quantum path control using attosecond pulse trains via UV-assisted resonance enhance ionization

Li Fang, Wei Lai, He Zhi-Cong
Chin. Phys. B . 2015, 24(4): 043301 . **doi:** 10.1088/1674-1056/24/4/043301

TOPICAL REVIEW — Strong-field atomic and molecular physics

Air lasing: Phenomena and mechanisms*

Helong Li(李贺龙)[1,2], Danwen Yao(姚丹雯)[2], Siqi Wang(王思琪)[2], Yao Fu(付尧)[2], and Huailiang Xu(徐淮良)[2,3,†]

[1] *Institute of Atomic and Molecular Physics, Jilin University, Changchun* 130012, *China*
[2] *State Key Laboratory of Integrated Optoelectronics, College of Electronic Science and Engineering, Jilin University, Changchun* 130012, *China*
[3] *State Key Laboratory of Precision Spectroscopy, East China Normal University, Shanghai* 200062, *China*

(Received 3 July 2019; revised manuscript received 29 August 2019; published online 25 October 2019)

Air lasing is a concept that refers to remote no-cavity (mirrorless) optical amplification in ambient air with the air constituents as the gain media. Due to the high potential of air lasing in view of applications in atmospheric sensing, a variety of pumping schemes have been proposed so far for building up population-inverted gain media in air and producing forward and/or backward directional lasing emissions. This review paper presents an overview of recent advances in the experimental observations and physical understanding of air lasing in various pumping schemes of air molecules by intense laser fields. Special emphasis is given to the strong-field-induced N_2^+ air lasing, the mechanism of which is currently still in a hot debate.

Keywords: air lasing, intense laser fields, nitrogen molecules

PACS: 42.65.Re, 33.20.Xx **DOI:** 10.1088/1674-1056/ab47f5

1. Introduction

Since the first ruby laser was demonstrated in 1960, there have been enormous requirements for a variety of coherent light sources in a broad spectrum of fields covering science and engineering.[1,2] In environmental science, there has been a large amount of research efforts aiming at measuring atmospheric trace species over a long distance. The ability to control the generation of coherent light source with different frequencies at a designated location would provide a new strategy to meet the pressing needs of various environmental issues from monitoring global warming and stratospheric ozone depletion to early detection of nuclear reactor radiation leak and biological treat agents in air.[3,4] Thanks to the rapid progress of high-power ultrafast laser technologies in the last two decades,[5] a so-called "air lasing" concept based on the filamentation of intense femtosecond laser pulses in air was proposed,[6] which provides the possibility for remote generation of no-cavity optical amplification in the population-inverted constituents of air at a desired distance.

Laser filamentation is a unique nonlinear optical phenomenon resulting from the propagation of powerful femtosecond laser pulses in transparent optical media.[7,8] In air, the laser intensity inside the filament core is clamped to a nearly constant value of 50–100 TW/cm^2,[9,10] which ranges from centimeters to tens of meters at a far distance.[11,12] The high-intensity laser field can induce ionization and fragmentation of molecules in the laser propagation path, giving rise to characteristic optical emissions from the ionized or fragmented molecules.[13–15] Interestingly, it was demonstrated that some of the ionized and fragmented particles from parent molecules such as N_2, CH_4, and H_2O inside the filament core can be populated inverted, resulting in amplification of incoherent (e.g., fluorescence) or coherent (e.g., supercontinuum or harmonics) light.[6,16–20] Since the high-intensity filament in air can be projected at a far distance and is hardly disturbed even in adverse environments,[21–23] creation of population-inverted air molecules by femtosecond laser filamentation has been regarded as a promising step towards the remote generation of bright directional radiation, called air lasing, in the atmosphere. Different from conventional laser schemes, air lasing is a concept that enables remote no-cavity (mirrorless) optical amplification in ambient air with the air constituents as the gain media, which holds three unique properties: (i) remote generation of optical gain in air molecules, (ii) no-cavity required for optical amplification, and (iii) incoherent/coherent directional radiation opposed to (backward) and/or along (forward) the pump laser propagation direction.

Air lasing was first proposed in the early 2000's by Chin's group from the observation of amplified spontaneous emission (ASE) in a femtosecond filament, in which the intensity of the backward scattered fluorescence from the $C^3\Pi_u$–$B^3\Pi_g$ transition of N_2 at 357 nm showed an exponential dependence on the input laser energy (filament length).[6] The optical gain was measured to be about 0.3 cm^{-1},[6] which showed a strong spatial dependence.[24] After the first observation of filament-induced ASE in air, such exponential increase of fluorescence

*Project supported by the National Natural Science Foundation of China (Grant Nos. 61625501, 61427816, and 11904121), the Open Fund of the State Key Laboratory of High Field Laser Physics (SIOM), China, the Program for JLU Science and Technology Innovative Research Team (JLUSTIRT), China (Grant No. 2017TD-21), and Fundamental Research Funds for the Central Universities of China.

†Corresponding author. E-mail: huailiang@jlu.edu.cn

© 2019 Chinese Physical Society and IOP Publishing Ltd

as a function of the filament length was subsequently observed for a number of fragmented molecules such as CH from the mixture of air and hydrocarbon molecules CH_4, C_2H_2, and C_2H_4,[18] and OH and NH from water vapor H_2O in air,[19,20] and CN from the ethanol–air flame.[25] Furthermore, narrowband lasing lines from backward or forward directions along the pump laser propagation path have been demonstrated with atomic oxygen (O) and nitrogen (N),[26–28] neutral and singly-ionized nitrogen molecules (N_2, N_2^+),[6,16,17] and ionized carbon oxides[29] as gain media.

In this review, we will present an overview of recent research progress in the experimental observations and physical understanding of air lasing in various pumping schemes. We will focus on air lasing produced from the two most abundant atmospheric constituents, i.e., nitrogen and oxygen molecules by intense laser fields, while for that from other molecules, the readers can refer to a few available review papers.[15,30,31] In addition, the discussion in this review will not only be limited to air lasing induced by femtosecond laser filamentation, but also include the air lasing phenomena produced at low gas pressure by strong laser field in the absence of laser filamentation. Different from the filamentation case where the clamping effect in the filamentation process limits the modulation of the laser intensity, the laser intensity in the latter case can be varied in a large range, so that many nonlinear optical effects in the filamentation regime could be excluded during the discussion of air lasing, providing a benefit in understanding of the underlying mechanism of air lasing induced by strong-field excitation. The context is organized as follows. We begin with the lasing actions observed from the O and N atoms with the pump of air molecules by intense picosecond/nanosecond laser pulses in the ultraviolet (UV) spectral range, which is followed by the introduction to recent progress in N_2 lasing driven by near-infrared femtosecond laser pulses. We then give an overview of N_2^+ lasing in a number of pumping schemes of N_2 molecules by near-infrared and mid-infrared intense laser fields, with a special emphasis on the understanding of its physical mechanism. Lastly, both current challenges and a future outlook are given.

2. Atomic air lasing pumped by deep-ultraviolet laser pulses

High optical gain on the transition between the 3p ^{3}P→ 3s ^{3}S levels of oxygen atoms in air induced by a 226-nm and 100-ps laser pulse was experimentally demonstrated in 2011 by detecting the forward and backward 845-nm emissions along the pump laser propagation.[26] The measured pulse duration of the backward-propagating 845-nm emissions is about 300 ps, which is two orders of magnitude shorter than the fluorescence lifetime (about 36 ns) of the 3p ^{3}P level.[32] The measured optical gain is larger than 60 cm^{-1}. The mechanism of the gain was ascribed to the two-photon dissociation of the oxygen molecules followed by two-photon-resonant pumping of the atomic oxygen fragments by the 226-nm intense laser light, as shown in Fig. 1(a). That is, the intense UV pump laser plays two roles in the generation of ASE-type oxygen air lasing: (i) dissociation of oxygen molecules, and (ii) building up the population inverted oxygen through two-photon excitation of the resultant oxygen atoms.

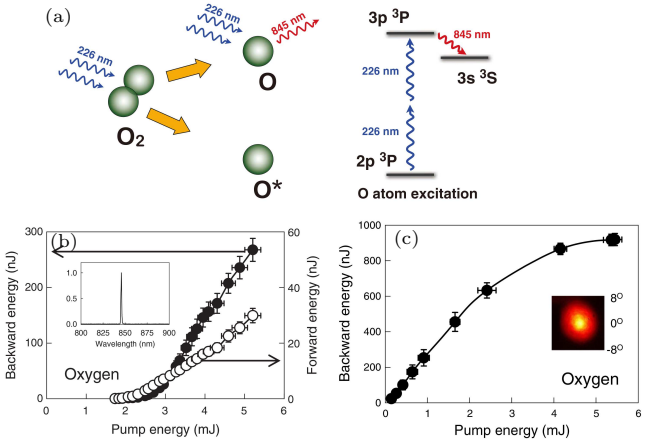


Fig. 1. (a) Schematic diagram for the oxygen atomic lasing pumped by the 266-nm laser.[26] (b) Energy output of the backward and forward air lasing in the absence of the dissociating pulse, and (c) that of the backward air lasing in the presence of the dissociating pulse, as a function of energy of the deep-UV pump pulse, for the case of atmospheric oxygen emission. Inset in (b): the spectrum of backward air lasing; and inset in (c): the far-field intensity profile of the generated backward-propagating laser beam.[33]

However, the threshold of atomic oxygen lasing induced by deep-UV pumping is as high as a few hundred of GW/cm^2,[26] which would limit the performance of this approach at a standoff range.[33] To lower or even eliminate the lasing threshold, a pre-dissociation air lasing scheme was proposed,[33] in which an additional nanosecond laser was used to dissociate air molecules, and then the resultant atomic oxygen and nitrogen were excited by a tunable deep UV laser source through two-photon absorption. In this experiment, both the dissociation and the pump laser sources were operated at the 6-ns pulse duration and repetition rate of 10 Hz. The dissociating pulse firstly generates neutral atomic fragments by the high-energy electron impact and after a few microseconds, the focused pumping pulse reaches the interaction zone to excite the atomic fragments, resulting in bidirectional coherent emissions. As an example, the thresholds of atomic oxygen lasing in the absence and presence of the dissociating pulse are shown in Figs. 1(b) and 1(c), respectively. The wavelength of the pump was set at 226 nm. Figure 1(b) clearly shows that when the dissociating laser is turned off, the thresholds of both the forward and backward lasing emissions at 845 nm (see inset of Fig. 1(b)) are high, in hundreds of GW/cm^2. While when the dissociating laser is turned on, it can be seen from Fig. 1(c) that the lasing threshold is significantly decreased, resulting in a virtual elimination of the lasing threshold that

is below the measurement uncertainty and thus cannot be reliably quantified.[33]

Similar experiments for atomic nitrogen air lasing were also performed by dissociating nitrogen molecules and subsequently pumping of the atomic nitrogen through two-photon excitation.[33] The low-threshold lasing of nitrogen atoms with the transitions between the 3p $^4D^0$ and 3s ^4P states at 870 nm and that between the 3p $^4S^0$ and 3s ^4P states at 745 nm were investigated with the 211 nm and 207 nm pump lasers, respectively. Low-threshold forward and backward emissions were achieved, showing that the approach is feasible for generating air lasing on a variety of transitions of oxygen and nitrogen atoms fragmented in air.[33]

3. N_2 and N_2^+ air lasing driven by intense laser fields

It is long known that the air molecules exposed to intense laser fields can give rise to characteristic optical emissions, which are mainly assigned to two spectral band systems: the second positive band system of N_2 ($C^3\Pi_u$–$B^3\Pi_g$ transition) and the first negative band system of N_2^+ ($B^2\Sigma_u^+$–$X^2\Sigma_g^+$ transition).[34] Recently, it has been demonstrated that the optical emissions from both N_2 and N_2^+ can be amplified inside the plasma channel, resulting in narrow-band lasing emissions.[6,16,17] In this section, we will overview the recent progress in N_2 and N_2^+ lasing driven by intense femtosecond laser pulses in various pumping schemes.

3.1. N_2 lasing actions

Since the first demonstration of the gain on the $C^3\Pi_u \rightarrow B^3\Pi_g$ transition of N_2 in an air filament by detecting the backward ASE,[6,35] a variety of pumping scenarios have been proposed for enhancing the N_2 lasing emissions, such as the gain-swept superradiance[36] and the "igniter-heater" configuration.[37–40] Experimentally, a significant enhancement of the backward ASE-type N_2 lasing driven by a mid-infrared femtosecond laser filament was then realized in an Ar–N_2 gas mixture.[41] The experiment was carried out at a distance above 2 m with mid-infrared, 4 μm wavelength pulses. By focusing the 80 fs/8 mJ mid-infrared laser pulses in the mixture of 1-bar N_2 and 5-bar Ar gas, backward lasing actions induced by filamentation of the laser pulses were unambiguously observed. Two strong narrow-bandwidth lines at 357 nm and 337 nm, assigned respectively to the $C^3\Pi_u$ ($v' = 0$)–$B^3\Pi_g$ ($v = 1$) and $C^3\Pi_u$ ($v' = 0$)–$B^3\Pi_g$ ($v = 0$) transitions, appeared in the backward spectrum (see Fig. 2(a)). These two lines are much narrower than the fluorescence bands,[34] showing a clear evidence of ASE-type lasing action. As shown in Fig. 2(b), the mechanism behind the population inversion in N_2 was attributed to resonant excitation transfer from the excited Ar atoms to N_2 molecules, where the excited Ar atoms are produced by a two-step collision process.[41] The measured output energy of the backward lasing emissions can reach to 3.5 μJ with an energy conversation efficiency of $\sim 0.5\%$, which could be employed for sensing trace species by stimulated Raman spectroscopy.[42]

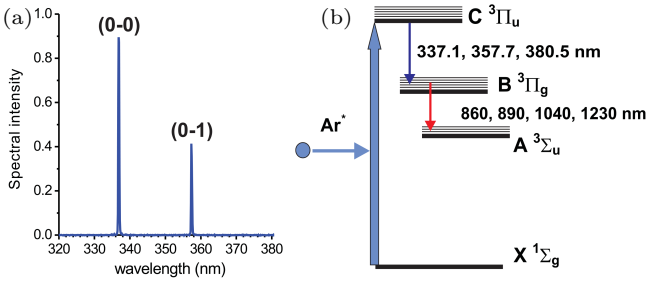


Fig. 2. (a) Spectra of backward lasing emissions from the 1 bar of N_2 and 5 bars of Ar mixture induced by filamentation of mid-infrared, 4 μm wavelength pulses at a distance above 2 m, and (b) excitation and energy-level diagram of the backward ASE-type N_2 lasing.[41]

The gain dynamics of the backward N_2 laser generated in an Ar–N_2 mixture were subsequently investigated based on pump–probe measurements using 800-nm femtosecond laser pulses.[43] After the creation of population inversion, the weak probe pulse reached the interaction zone to quench the N_2 lasing signal by kicking off N_2 molecules from the state $C^3\Pi_u$. The gain duration could be finely tuned by changing the delay between the pump and the probe. It was demonstrated that the minimum gain duration of about 0.8 ns is required under this experimental condition for the occurrence of the backward lasing signal by comparing the gain dynamics between the forward and backward lasing actions.[43]

The generation of the intense backward N_2 lasing emission in the circularly-polarized femtosecond laser fields was also demonstrated.[44,45] Figure 3(a) shows backward emission spectra of the pure N_2 gas induced by circular- and linear-polarized laser filaments (800 nm/50 fs/9.3 mJ) at the atmospheric pressure.[44] It can be seen that the 337-nm spectral intensity in the circularly-polarized case is higher by one order of magnitude than that in the linearly-polarized case. By changing the angle of optic axis of the quarter wave plate, it was found that the 337-nm signal intensity decreases dramatically as the laser polarization state varies from circular to linear, as shown in Fig. 3(b).

The dramatic enhancement of backward N_2 fluorescence in the circularly-polarized laser field was explained based on the ASE phenomenon with the population inversion of N_2 induced by the inelastic electron impact excitation.[44,45] To verify this, the electron kinetic energy distributions in the linearly- and circularly-polarized laser fields were calculated, as shown in Figs. 3(c) and 3(d), respectively.[46] In the linearly-polarized laser fields, the kinetic energy distribution reveals that most electrons produced by ionization of N_2 have the energy below 1 eV, while in the circularly-polarized laser

field, the electrons produced from the photon ionization would be further accelerated by the laser field, leading to the higher kinetic energy with the distribution peaked at $\sim$ 14.6 eV. The produced high-energy electrons in the circularly-polarized case enable more efficient excitation of N_2 from the ground $X^1\Sigma_g$ state to the $C^3\Pi_u$ state than to the $B^3\Pi_g$ state due to the larger collision cross section of the $X^1\Sigma_g$–$C^3\Pi_u$ transition in the energy range of 10–20 eV.[47]

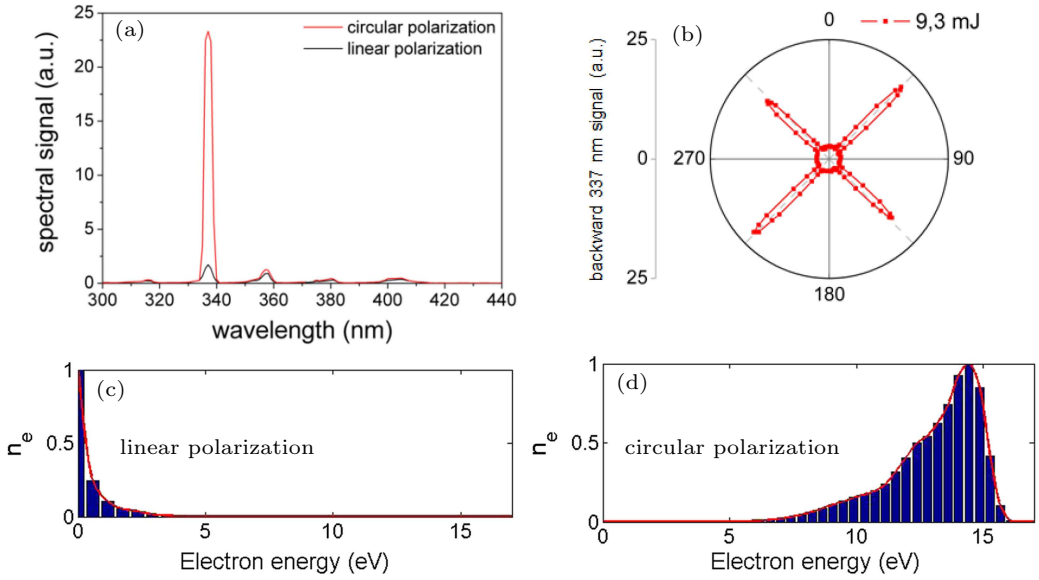


Fig. 3. (a) Spectra of backward N_2 emission for the circular (red) and linear (black) laser polarizations, at 9.3-mJ pulse energy, (b) the 337-nm emission signal vs. the rotation angle of the quarter wave plate, where the angle 0° corresponds to linearly polarized light.[44] (c) and (d) Calculated electron energy distributions in the cases of (c) linearly and (d) circularly polarized laser pulses at the laser intensity of 1.4×10^{14} W/cm^2.[46]

It was further confirmed that the population inversion of N_2 was indeed established in the circularly-polarized laser field by investigating the external seeded lasing action of N_2 molecules in the forward and backward directions.[48–51] However, the lasing intensity and pulse duration showed obvious difference behaviors for the forward and backward conditions, which may result from the finite gain lifetime and the traveling excitation scheme as well as the temporal dynamics of the electron–neutral collisions.[50,51]

It should be emphasized that O_2 molecules play a negative role in the N_2 lasing actions in air due to the collision reaction N_2 $(C^3\Pi_u)+ O_2 = N_2$ $(X^1\Sigma_g)+ O + O$, which leads to a significant reduction of the N_2 population on the $C^3\Pi_u$ state.[52] It was demonstrated that when the concentration of O_2 molecules exceeds 15% in the mixture of N_2 and O_2 gas, with the pumping of 9.3 mJ incident laser energy, the intensity of the backward 337-nm emission of N_2 by the circularly polarized light is reduced to the level close to that obtained by the linearly-polarized laser.[44]

Recently, the forward N_2 coherent emission at 337 nm was also investigated in the pure N_2 gas or in ambient air using a linearly-polarized picosecond laser pulse (1053 nm/10 ps/10 J).[53] When the laser pulse was focused in air to form an air filament, third harmonic (TH) was generated, whose spectrum covers the transition between the $C^3\Pi_u$ $(v' = 0)$ and $B^3\Pi_g$ $(v = 0)$ states. Harmonic-seeded amplification occurred, giving rise to a strong forward lasing emission at 337 nm. The population inversion between the $C^3\Pi_u$ and $B^3\Pi_g$ states in N_2 was ascribed to the collision excitation by the hot electrons generated during the laser-induced breakdown of air molecules. It should be pointed out that with this pumping scheme, since the gain medium was seeded by the TH of the pump laser, the lasing emission occurred on the timescale defined by the incident laser duration of 10 ps.

3.2. N_2^+ lasing actions

Another important research topic in air lasing is the forward lasing in N_2^+ induced by strong-laser pulses. In 2011, it was observed that forward high-brightness narrowband emissions at 330 nm, 357 nm, 391 nm, 428 nm, and 471 nm, corresponding to different vibrational transitions between the $B^2\Sigma_u^+$ and $X^2\Sigma_g^+$ states, can be achieved by producing a filament in air using a wavelength-tunable optical parametric amplifier (OPA) laser system.[16] This phenomenon was ascribed to ultrafast establishment of population-inverted N_2^+ by strong laser fields, followed by the amplification of the self-generated harmonic seed in the filament.[16,54] However, in the strong-field ionization theory, it is commonly accepted that the ionization would leave most of ionized nitrogen molecules on the ground state.[55–58] Since the above observation was seemingly contradictory to the strong-field theory, considerable effort has been made to clarify the mechanism responsible for the narrow-band forward emissions of N_2^+ induced by strong laser fields.

Since in the self-generated harmonic seed scheme,[16] the self-generated harmonic in the filament is temporally overlapped with the mid-infrared driven laser, the delay time between the pump and the self-generated seed cannot be easily modified, making it difficult to examine the dynamics of lasing emission of N_2^+. Therefore, the coherent emission of N_2^+ was subsequently investigated based on a pump–probe scheme, in which the 800-nm fundamental light from a Ti: sapphire laser system was employed as the pump to prepare the population inversion in N_2^+ and its second harmonic generated by frequency-doubling was used as the probe to be amplified.[59] By manipulating the propagating direction of the pump and the probe, spectral property, and intensity of the probe pulse, some parametric processes such as four-wave mixing and stimulated Raman scattering were excluded as the origin of coherent N_2^+ emissions at the 800 nm pump condition, and the population inversion was regarded as the most possible mechanism.[60] By measuring the forward externally-injected seed-amplification lasing spectra, one could obtain much information such as gain dynamics[61–64] and remote characterization of rotation coherence,[65] and population densities and dynamics in different rotational levels,[66–71] which is significant for understanding the mechanism behind the establishment of the optical gain and achieving the coherent control of the N_2^+ lasing.[72–75]

The above mentioned OPA laser has a low laser energy output, making it hard to generate a filament at a remote location, while the pump–probe scheme has a difficulty to temporally and spatially overlap the two pulses over a far distance. A variety of pumping schemes for generation of N_2^+ air lasing have been proposed to overcome the above drawbacks.[17,76–82] For example, it was demonstrated that the N_2^+ lasing emissions could be generated using a single 800-nm Ti: sapphire femtosecond laser pulse, in which the self-generated white-light produced by self-phased modulation served as the seed,[17,76–81] and the laser energy output up to micro-joule level for the $B^2\Sigma_u^+$ ($v'=0$)$\rightarrow X^2\Sigma_g^+$ ($v=1$) transition at 428 nm was realized.[81] In addition, in order to overcome strong signal fluctuation of air lasing introduced by the self-generated white light, a co-axial dual-color femtosecond laser field (800 nm fundamental laser and its second harmonic) was proposed to generate air lasing at extended distances. In this case, the dual-color laser field was generated by inserting a barium borate crystal in the propagation path of the 800-nm fundamental Ti: sapphire pump laser pulse,[82] and the N_2^+ lasing in air was unambiguously achieved, as shown in Fig. 4. The inset of Fig. 4 shows that the lasing signal has a nearly linear polarization that is parallel to that of the 400 nm seed.

It should be pointed out that even though the N_2^+ lasing actions induced by strong-light excitation has been extensively investigated in the past decade, the physical mechanism responsible for the population inversion of N_2^+ is still hot discussed with a variety of physical pictures, such as field-induced multiple recollision,[83,84] post-ionization multiple-state coupling,[85–87] transient inversion due to rotation coherence,[88] different rotational distributions between two states,[89] and near-resonant Raman amplification.[90–92] Here we will only focus our discussion on the contributions from field-induced multiple recollision[83,84] and post-ionization multiple-state coupling,[85–87] which have attracted more attention among the above proposed scenarios.

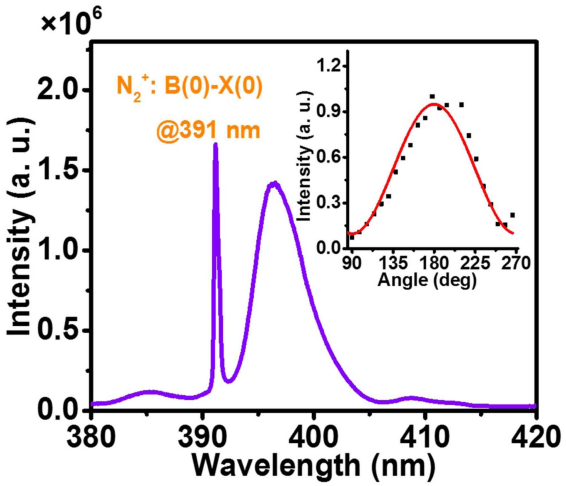


Fig. 4. Forward lasing spectrum produced by a coaxial 800 nm+400 nm laser pulse in air. Inset shows the measured (dot) and fitted (solid line) coherent characteristics of the narrowband signal at 391 nm.[82]

In 2015, it was proposed, by comparing the ellipticity effect of the pump laser on air lasing with that of high-order harmonic generation (HHG),[93] that the field-induced multiple electron recollisions could play an essential role in achieving the optical gain of N_2^+.[83,84] In this scheme, in the linearly polarized pulse case, after tunnel ionization the electrons driven by the laser field move back and interact with the parent ion by inelastical impact, leading to efficient transfer of the N_2^+ population from the ground $X^2\Sigma_g^+$ state to the excited $B^2\Sigma_u^+$ state, and creating the gain on the $B^2\Sigma_u^+$–$X^2\Sigma_g^+$ transition of N_2^+. It was further demonstrated that the N_2^+ lasing intensity was extremely sensitive to the duration and wavelength of the driven laser pulses, which was ascribed to the interference of dipolar moments of N_2^+ created by electron recollisions.[94]

However, by reexamining the ellipticity effect of the pump laser on air lasing under different conditions,[95] it was recently demonstrated that the N_2^+ gain and HHG behave differently as the ellipticity of the driven pulse changes, from which it was concluded that the electron recollision does not play a dominant role in building up the population inversion of N_2^+.[95] More recently, the 428-nm lasing action of N_2^+ was investigated by using a bicircular two-color (BTC) femtosecond laser pulse,[96] and similar lasing results were observed for the

co-rotating and the counter-rotating BTC driving fields. Since the field-induced electron recollision is suppressed in the co-rotating BTC field as compared to that in the counter-rotating field, it was also concluded that the electronic impact makes a minor contribution to the population inversion of N_2^+. The controversial issue of the above mentioned recollision mechanism for N_2^+ air lasing remains to be understood.

Meanwhile, a pumping scheme based on post-ionization multiple-state coupling, as shown in Fig. 5(a), was also proposed in 2015.[85,86] In this scheme, after the strong-field ionization by the most strongest central part of the pulse, the rear part of the laser induces multiple state couplings among the lowest three states, $X^2\Sigma_g^+$, $A^2\Pi_u$, and $B^2\Sigma_u^+$ of N_2^+, which enable efficient depletion of the population on the $X^2\Sigma_g^+$ state, resulting in gain on the $B^2\Sigma_u^+$–$X^2\Sigma_g^+$ transition of N_2^+. Figure 5(b) shows a typical lasing spectrum induced in air by few-cycle laser pulses (6 fs/0.2 mJ/800 nm). The white light produced from self-phased modulation serves as the seed to be amplified in the population-inverted N_2^+ system, resulting in the forward coherent emission at 391 nm. With the above experimental conditions, the numerical simulation of multiple state coupling was performed. As shown in Fig. 5(c), the theoretical results of the time-dependent populations on the three electronic states suggest that the intermediate state $A^2\Pi_u$ serves as the population reservoir to accept the population transferred from the ground state.[85] The effects of the pulse duration[85] and the wavelength[86] on the post-ionization coupling were also investigated.

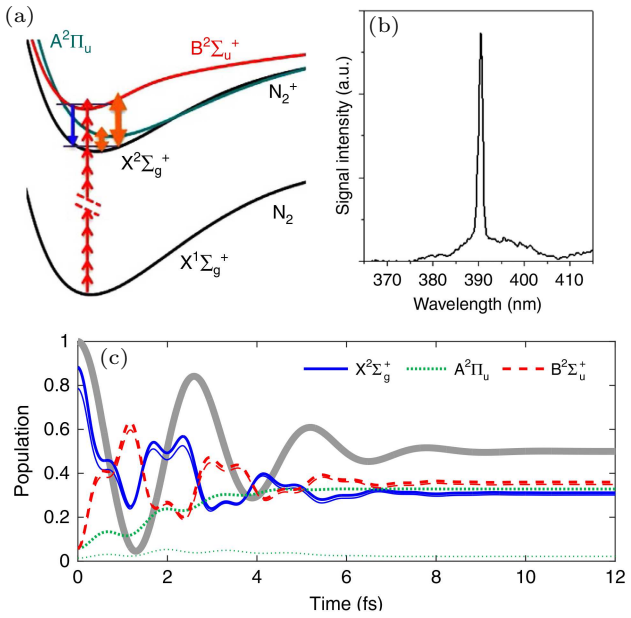


Fig. 5. (a) Schematics of the ionization and coupling concept for the population inversion in N_2^+, (b) forward spectrum of air lasing induced by a few-cycle laser pulse, and (c) numerical simulation of time-dependent populations in the three electronic states, in which the few-cycle laser field (grey curve) is presented for comparison.[85]

Interestingly, the coupling model[85] can well explain the molecular alignment effect on the N_2^+ lasing,[97] in which the N_2 molecules were first aligned by a weak laser pulse (50 fs/800 nm/34 μJ) and then pumped by a strong few-cycle laser pulse (6.3 fs/800 nm/49 μJ). As shown in Fig. 6 (a), the intensity of the generated lasing emission at 391 nm could be enhanced or suppressed by finely adjusting the delay time τ between the alignment pulse and the pumping pulse whose polarization directions were set to be parallel with each other. In addition, the lasing intensity (Fig. 6(b)) showed a cosine dependence on the angle α of the polarization direction of the alignment pulse with respect to that of the pumping pulse. It was discussed that the modulation of the lasing signals is not from other effects such as the change in nonlinear refractive index induced by the molecular alignment.[97] As shown by the red lines in Fig. 6, numerical simulation based on the model of post-ionization light-induced coupling combined with the time-dependent rotational motion of N_2 reproduced the experimental results, which supports the idea that the post-ionization multiple-state coupling effect plays an essential role in building up the population inversion between the $B^2\Sigma_u^+$ and $X^2\Sigma_g^+$ states of N_2^+.

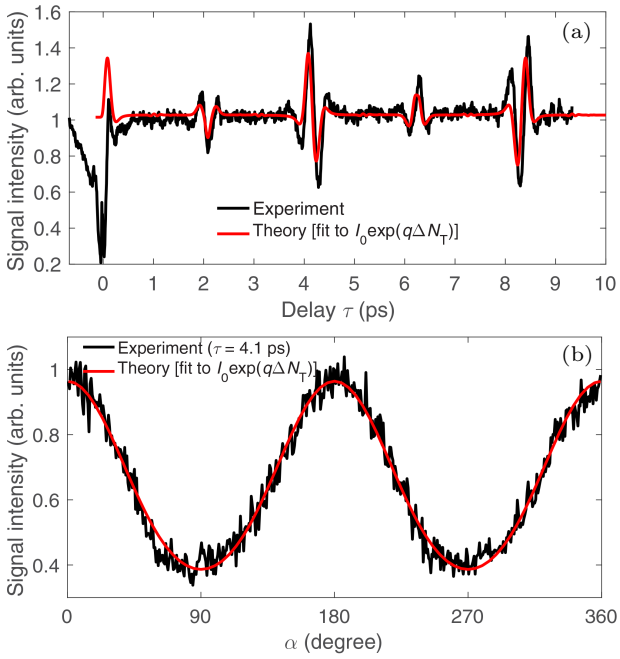


Fig. 6. (a) Measured (black line) and simulated (red line) 391-nm lasing intensity as a function of the delay time τ between the alignment and pumping pulses, and (b) measured and simulated 391-nm lasing intensity as a function of the angle α between the polarization direction of the alignment pulse and that of the pumping pulse.[97]

It is known that the ionization of N_2 preferentially occurs when the molecular axis is parallel to the polarization direction of the driven laser polarization due to the orbit symmetry,[98] but in the coupling model the optical coupling between the $A^2\Pi_u$ and $X^2\Sigma_g^+$ states would be more efficient when the molecular axis is perpendicular to the polarization direction of the driven laser polarization due to the perpendicular transition. Therefore, it was expected that the lasing intensity of N_2^+ would be sensitive to the polarization state of the rear part

of the driven laser.[99] Recently, the post-ionization coupling effect on the N_2^+ lasing was investigated[99] using an intense laser pulse, whose polarization can be modulated in time by a so-called polarization gating (PG) technique.[100] With the PG setup shown in Fig. 7(a) to modulate the polarization state of the laser pulse, a significant enhancement of the lasing intensity was observed in the PG pulse case, as compared with that in the linearly-polarized pulse case. In contrast, under the same experimental condition, fluorescence measurement revealed that the population on the excited state $B^2\Sigma_u^+$ in the PG laser field is lower than that of linearly polarized pulse. The enlarged gain was ascribed to the stronger coupling between the ground state $X^2\Sigma_g^+$ and the intermediate state $A^2\Pi_u$ due to the existence of the perpendicular laser part in the PG pulse, which made an efficient population transfer from $X^2\Sigma_g^+$ to $A^2\Pi_u$. Numerical simulations based on the coupling model reproduced the experimental results.

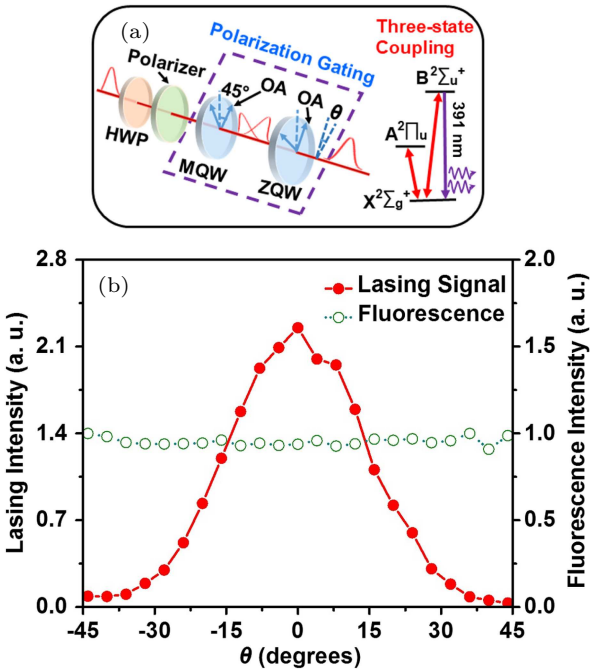


Fig. 7. (a) Schematic diagram of the polarization gating, where HWP stands for a half wave plate, and OA is the optical axis of the multiple order quarter wave plate (MQW) and that of the zero-order quarter wave plate (ZQW). The angle θ is the angle between the OAs of MQW and ZQW. (b) The intensity of the 391-nm lasing (filled red circle) and that of the 391-nm fluorescence (open green circle) induced by the polarization-modulated pulses.[99]

Furthermore, it was found that the lasing and fluorescence emission signals showed different dependences on the ellipticity of the rear part of the pumping laser, as shown in Fig. 7(b). The constant intensity of the fluorescence was ascribed to the constant population in the excited $B^2\Sigma_u^+$ state in the entire range of θ, implying that the ionization only occurs in the central part of the PG pulse, and is not sensitive to the polarization state of the rear part of the pumping laser pulse. The constant fluorescence also implies that the collisional excitation by free electrons is negligible in the PG case. Since the population on the excited $B^2\Sigma_u^+$ state keeps constant, the dramatic variation in the intensity of N_2^+ lasing means that the population on the ground state is efficiently depleted by the PG pulse, supporting that the light-induced coupling effect after tunnel ionization indeed plays key roles in establishing the population inversion of N_2^+.

4. Summary and prospective

In this article, we have presented results of recent studies on lasing actions in air induced by intense laser pulses in a variety of pumping schemes. This dynamical research field was stimulated by the experimental observation of ASE produced during filamentation of femtosecond laser pulses propagating in air. Since the filamentation can project a 50–100 TW/cm^2 laser intensity at a designated far distance holding high potential for remote atmospheric sensing, air lasing is referred as to an efficient method to greatly increase the signal-to-noise ratio in the filamentation remote sensing scheme.

We have introduced several representative gain media including oxygen and nitrogen atoms, and neutral and ionized nitrogen molecules, and also discussed their generation mechanisms. To date, the physics behind the population inversion of atomic oxygen and nitrogen induced in air by deep-UV laser pulses, as well as that of neutral nitrogen molecules by near-infrared intense laser fields are almost clear, but the underlying mechanism of building up population-inverted N_2^+ lasing by intense near- and mid-infrared fields, which could not be naturally achieved by strong-field ionization, is still in a hot debate. In the recent discussion of the N_2^+ lasing mechanisms, special attention has been given to the field-induced recollision and multiple state coupling, both of which are the post-ionization processes.

Although air lasing has been regarded as a promising tool in atmospheric applications for detection of, e.g., molecular rotational coherence,[65] and stimulated Raman scattering,[42,101] the practical application of air lasing is still a big challenge and strongly depends on the progress in the following research subjects: (i) understanding mechanisms of strong-field–molecule interaction for building up population-inverted atmospheric constituents in various atmospheric conditions, (ii) generating high-power output of air lasing over a long distance, (iii) generating backward air lasing with different atmospheric constituents as gain media. In particular, the backward air lasing would be a key factor for the detection of remote targets in the practical application. Novel experimental scenarios and technologies are expected to control the gain dynamics of light in the backward direction, for example, using a newly developed technique called "flying focus",[102] which can make the laser focus counter-propagate along the laser axis.

References

[1] Maiman T H 1960 *Nature* **187** 493
[2] Demtroder W 2011 *Laser Spectroscopy: Basic Concepts And Instrumentation* (3rd Edn) (Berlin: Springer)
[3] Schiff H I, Mackay G I and Bechara J 1994 *The Use Of Tunable Diode Laser Absorption Spectroscopy For Atmospheric Measurements*, In *Air Monitoring By Spectroscopic Techniques* (Sigrist M, Ed.) (New York: Wiley) pp. 239–335
[4] Svanberg S 1994 *Differential Absorption Lidar (DIAL)*, In *Air Pollution Monitoring With Optical Techniques* (Sigrist M, Ed.) (New York: Wiley) pp. 85–162
[5] Rulliere C 2005 *Femtosecond Laser Pulses* (Springer Science Business Media, Incorporated)
[6] Luo Q, Liu W and Chin S L 2003 *Appl. Phys. B* **76** 337
[7] Couairon A and Mysyrowicz A 2007 *Phys. Rep.* **441** 47
[8] Chin S L 2010 *Femtosecond Laser Filamentation* (Vol. **55** of Springer Series on Atomic, Optical and Plasma Physics)
[9] Liu W 2014 *Chin. J. Phys.* **52** 465
[10] Liu X L, Cheng W, Petrarca M and Polynkin P 2016 *Opt. Lett.* **41** 4751
[11] Chen Y, Théberge F, Kosareva O, Panov N, Kandidov V P and Chin S L 2007 *Opt. Lett.* **32** 3477
[12] Daigle J F, Kosareva O, Panov N, Wang T J, Hosseini S, Yuan S, Roy G and Chin S L 2011 *Opt. Commun.* **284** 3601
[13] Xu H L and Chin S L 2011 *Sensors* **11** 32
[14] Yuan S, Chin S L and Zeng H P 2015 *Chin. Phys. B* **24** 014208
[15] Xu H L, Cheng Y, Chin S L and Sun H B 2015 *Laser Photon. Rev.* **9** 275
[16] Yao J, Zeng B, Xu H, Li G, Chu W, Ni J, Zhang H, Chin S L, Cheng Y and Xu Z 2011 *Phys. Rev. A* **84** 051802
[17] Wang T, Ju J, Daigle J F, Yuan S, Li R and Chin S L 2013 *Laser Phys. Lett.* **10** 125401
[18] Hosseini S, Azarm A, Daigle J F, Kamali Y and Chin S L 2014 *Opt. Commun.* **316** 61
[19] Yuan S, Wang T J, Teranishi Y, Sridharan A, Lin S H, Zeng H P and Chin S L 2013 *Appl. Phys. Lett.* **102** 224102
[20] Yuan S, Wang T J, Lu P F, Chin S L and Zeng H P 2014 *Appl. Phys. Lett.* **104** 091113
[21] Chin S L, Talebpour A, Yang J, Petit S, Kandidov V P, Kosareva O G and Tamarov M P 2002 *Appl. Phys. B* **74** 67
[22] Méjean G, Kasparian J, Yu J, Salmon E, Frey S, Wolf J P, Skupin S, Vinçotte A, Nuter R, Champeaux S and Bergé L 2005 *Phys. Rev. E* **72** 026611
[23] Salamé R, Lascoux N, Salmon E, Kasparian J and Wolf J P 2007 *Appl. Phys. Lett.* **91** 171106
[24] Zeng T, Zhao J Y, Liu W and Chin S L 2014 *Laser Phys. Lett.* **11** 075401
[25] Chu W, Li H, Ni J, Zeng B, Yao J, Zhang H, Li G, Jing C, Xie H, Xu H L, Yamanouchi K and Cheng Y 2014 *App. Phys. Lett.* **104** 091106
[26] Dogariu A, Michael J B, Scully M O and Miles R B 2011 *Science* **331** 442
[27] Traverso A J, Sanchez-Gonzalez R, Yuan L, Wang K, Voronine D V, Zheltikov A M, Rostovtsev Y, Sautenkov V A, Sokolov A V, North S W and Scully M O 2012 *Proc. Natl. Acad. Sci. USA* **109** 15185
[28] Dogariu A and Miles R B 2013 *in Frontiers in Optics, 2013/Laser Science XXIX*, Orlando, Florida, 2013 (Laser Science, Orlando, 2013)
[29] Chu W, Zeng B, Yao J, Xu H, Ni J, Li G, Zhang H, He F, Jing C, Cheng Y and Xu Z 2012 *Europhys. Lett.* **97** 64004
[30] Chin S L and Xu H L 2015 *Chin. Phys. B* **24** 013301
[31] Chin S L, Xu H L, Cheng Y, Xu Z Z and Yamanouchi K 2013 *Chin. Opt. Lett.* **11** 013201
[32] Aldén M, Westblom U and Goldsmith J E M 1989 *Opt. Lett.* **14** 305
[33] Laurain A, Scheller M and Polynkin P 2014 *Phys. Rev. Lett.* **113** 253901
[34] Talebpour A, Abdel-Fattah M, Bandrauk A D and Chin S L 2001 *Laser Phys.* **11** 68
[35] Owada S, Azarm A, Hosseini S, Iwasaki A, Chin S L and Yamanouchi K 2013 *Chem. Phys. Lett.* **581** 21
[36] Kocharovsky V, Cameron S, Lehmann K, Lucht R, Miles R, Rostovtsev Y, Warren W, Welch G R and Scully M O 2005 *Proc. Natl. Acad. Sci. USA* **102** 7806
[37] Hemmera P R, Milesb R B, Polynkinc P, Sieberta T, Sokolova A V, Spranglee P and Scully M O 2011 *Proc. Natl. Acad. Sci. USA* **108** 3130
[38] Sprangle P, Peñano J, Hafizi B, Gordon D and Scully M 2011 *Appl. Phys. Lett.* **98** 211102
[39] Peñano J, Sprangle P, Hafizi B, Gordon D, Fernsler R and Scully M 2012 *J. Appl. Phys.* **111** 033105
[40] Kartashov D and Shneider M N 2017 *J. Appl. Phys.* **121** 113303
[41] Kartashov D, Ališauskas S, Andriukaitis G, Pugžlys A, Shneider M, Zheltikov A, Chin S L and Baltuška A 2012 *Phys. Rev. A* **86** 033831
[42] Malevich P N, Maurer R, Kartashov D, Ališauskas S, Lanin A A, Zheltikov A M, Marangoni M, Cerullo G, Baltuška A and Pugžlys A 2015 *Opt. Lett.* **40** 2469
[43] Xie H Q, Li G H, Chu W, Zeng B, Yao J P, Jing C R, Li Z T and Cheng Y 2015 *New J. Phys.* **17** 073009
[44] Mitryukovskiy S, Liu Y, Ding P J, Houard A and Mysyrowicz A 2014 *Opt. Express* **22** 12750
[45] Li Z, Chu W, Zeng B, Yao J, Li G, Xie H, Wang Z and Cheng Y 2016 *J. Phys. B* **49** 065602
[46] Mitryukovskiy S, Liu Y, Ding P, Houard A, Couairon A and Mysyrowicz A 2015 *Phys. Rev. Lett.* **114** 063003
[47] Itikawa Y 2006 *J. Phys. Chem. Ref. Data* **35** 31
[48] Ding P, Mitryukovskiy S, Houard A, Oliva E, Couairon A, Mysyrowicz A and Liu Y 2014 *Opt. Express* **22** 29964
[49] Yao J, Xie H, Zeng B, Chu W, Li G, Ni J, Zhang H, Jing C, Zhang C, Xu H, Cheng Y and Xu Z 2014 *Opt. Express* **22** 19005
[50] Ding P, Oliva E, Houard A, Mysyrowicz A and Liu Y 2016 *Phys. Rev. A* **94** 043824
[51] Ding P, Escudero J C, Houard A, Sanchis A, Vera J, Vicéns S, Liu Y and Oliva E 2017 *Phys. Rev. A* **96** 033810
[52] Kunabenchi R S, Gorbal M R and Savadatti M I 1984 *Prog. Quant. Electron.* **9** 259
[53] Kartashov D, Ališauskas S, Baltuška A, Schmitt-Sody A, Roach W and Polynkin P 2013 *Phys. Rev. A* **88** 041805
[54] Ni J, Chu W, Zhang H, Jing C, Yao J, Xu H, Zeng B, Li G, Zhang C, Chin S, Cheng Y and Xu Z 2012 *Opt. Express* **20** 20970
[55] Becker A, Bandrauk A D and Chin S L 2001 *Chem. Phys. Lett.* **343** 345
[56] Lofthus A and Krupenie P H 1977 *J. Phys. Chem. Ref. Data* **6** 113
[57] Zhao S F, Jin C, Le A T, Jiang T F and Lin C D 2010 *Phys. Rev. A* **81** 033423
[58] Zhang H, Jing C, Li G, Xie H, Yao J, Zeng B, Chu W, Ni J, Xu H and Cheng Y 2013 *Phys. Rev. A* **88** 063417
[59] Yao J, Li G, Jing C, Zeng B, Chu W, Ni J, Zhang H, Xie H, Zhang C, Li H, Xu H, Chin S L, Cheng Y and Xu Z 2013 *New J. Phys.* **15** 023046
[60] Ni J, Chu W, Jing C, Zhang H, Zeng B, Yao J, Li G, Xie H, Zhang C, Xu H, Chin S, Cheng Y and Xu Z 2013 *Opt. Express* **21** 8746
[61] Li G, Jing C, Zeng B, Xie H, Yao J, Chu W, Ni J, Zhang H, Xu H, Cheng Y and Xu Z 2014 *Phys. Rev. A* **89** 033833
[62] Miao Z, Zhong X, Zhang L, Zheng W, Gao Y, Liu Y, Jiang H, Gong Q and Wu C 2018 *Phys. Rev. A* **98** 033402
[63] Zhong X, Miao Z, Zhang L, Jiang H, Liu Y, Gong Q and Wu C 2018 *Phys. Rev. A* **97** 033409
[64] Arissian L, Kamer B, Rastegari A, Villeneuve D M and Diels J C 2018 *Phys. Rev. A* **98** 053438
[65] Zhang H, Jing C, Yao J, Li G, Zeng B, Chu W, Ni J, Xie H, Xu H, Chin S, Yamanouchi K, Cheng Y and Xu Z 2013 *Phys. Rev. X* **3** 041009
[66] Lei M, Wu C, Zhang A, Gong Q and Jiang H 2017 *Opt. Express* **25** 4535
[67] Zhong X, Miao Z, Zhang L, Liang Q, Lei M, Jiang H, Liu Y, Gong Q and Wu C 2017 *Phys. Rev. A* **96** 043422
[68] Xu B, Jiang S, Yao J, Chen J, Liu Z, Chu W, Wan Y, Zhang F, Qiao L, Lu R, Cheng Y and Xu Z 2018 *Opt. Express* **26** 13331
[69] Xie H, Zeng B, Li G, Chu W, Zhang H, Jing C, Yao J, Ni J, Wang Z, Li Z and Cheng Y 2014 *Phys. Rev. A* **90** 042504
[70] Zeng B, Chu W, Li G, Yao J, Zhang H, Ni J, Jing C, Xie H and Cheng Y 2014 *Phys. Rev. A* **89** 042508
[71] Wang P, Wu C, Lei M, Dai B, Yang H, Jiang H and Gong Q 2015 *Phys. Rev. A* **92** 063412
[72] Chen J M, Yao J P, Zhang H S, Liu Z X, Xu B, Chu W, Qiao L L, Wang Z H, Fatome J, Faucher O, Wu C Y and Cheng Y 2018 arXiv preprint arXiv:1808.03914
[73] Zhang A, Liang Q, Lei M, Yuan L, Liu Y, Fan Z, Zhang X, Zhuang S, Wu C, Gong Q and Jiang H 2019 *Opt. Express* **27** 12638
[74] Zhang A, Lei M, Gao J, Wu C, Gong Q and Jiang H 2019 *Opt. Express* **27** 14922

[75] Clerici M, Bruhács A, Faccio D, Peccianti M, Spanner M, Markov A, Schmidt B E, Ozaki T, Légaré F, Vidal F and Morandotti R 2019 *Phys. Rev. A* **99** 053802
[76] Chu W, Li G, Xie H, Ni J, Yao J, Zeng B, Zhang H S, Jing C R, Xu H L, Cheng Y and Xu Z 2014 *Laser Phys. Lett.* **11** 015301
[77] Liu Y, Brelet Y, Point G, Houard A and Mysyrowicz A 2013 *Opt. Express* **21** 22791
[78] Wang T J, Daigle J F, Ju J, Yuan S, Li R and Chin S L 2013 *Phys. Rev. A* **88** 053429
[79] Jing C, Zhang H, Chu W, Xie H, Ni J, Zeng B, Li G, Yao J, Xu H, Cheng Y and Xu Z 2014 *Opt. Express* **22** 3151
[80] Jing C, Xie H, Li G, Zeng B, Chu W, Zhang H, Ni J, Yao J, Xu H, Cheng Y and Xu Z 2015 *Laser Phys. Lett.* **12** 015301
[81] Point G, Liu Y, Brelet Y, Mitryukovskiy S, Ding P, Houard A and Mysyrowicz A 2014 *Opt. Lett.* **39** 1725
[82] Li H, Zang H, Su Y, Fu Y and Xu H 2017 *J. Opt.* **19** 124006
[83] Liu Y, Ding P, Lambert G, Houard A, Tikhonchuk V and Mysyrowicz A 2015 *Phys. Rev. Lett.* **115** 133203
[84] Tikhonchuk V T, Tremblay-Bugeaud J F, Liu Y, Houard A and Mysyrowicz A 2017 *Eur. Phys. J. D* **71** 292
[85] Xu H, Lötstedt E, Iwasaki A and Yamanouchi K 2015 *Nat. Commun.* **6** 8347
[86] Yao J, Jiang S, Chu W, Zeng B, Wu C, Lu R, Li Z, Xie H, Li G, Yu C, Wang Z, Jiang H, Gong Q and Cheng Y 2016 *Phys. Rev. Lett.* **116** 143007
[87] Zhang Y, Lötstedt E and Yamanouchi K 2019 *J. Phys. B* **52** 055401
[88] Kartashov D, Haessler S, Ališauskas S, Andriukaitis G, Pugžlys A, Baltuška A, Möhring J, Starukhin D, Motzkus M, Zheltikov A M, Richter M, Morales F, Smirnova O, Ivanov M Y and Spanner M 2016 *Research in Optical Sciences* (Washington, DC: Optical Society of America) paper HTh4B.5
[89] Azarm A, Corkum P and Polynkin P 2017 *Phys. Rev. A* **96** 051401
[90] Yao J, Chu W, Liu Z, Xu B, Chen J and Cheng Y 2018 *New J. Phys.* **20** 033035
[91] Liu Z, Yao J, Chen J, Xu B, Chu W and Cheng Y 2018 *Phys. Rev. Lett.* **120** 083205
[92] Yao J, Chu W, Liu Z, Chen J, Xu B and Cheng Y 2018 *Appl. Phys. B* **124** 73
[93] Corkum P B 1993 *Phys. Rev. Lett.* **71** 1994
[94] Liu Y, Ding P, Ibrakovic N, Bengtsson S, Chen S, Danylo R, Simpson E R, Larsen E W, Zhang X, Fan Z Q, Houard A, Mauritsson J, L'Huillier A, Arnold C L, Zhuang S, Tikhonchuk V and Houard A 2017 *Phys. Rev. Lett.* **119** 203205
[95] Britton M, Laferrière P, Ko D H, Li Z, Kong F, Brown G, Naumov A, Zhang C, Arissian L and Corkum P B 2018 *Phys. Rev. Lett.* **120** 133208
[96] Li H, Song Q, Yao J, Liu Z, Chen J, Xu B, Kang Lin, Qiang J, He B, Xu H, Cheng Y, Zeng H and Wu J 2019 *Phys. Rev. A* **99** 053413
[97] Xu H, Lötstedt E, Ando T, Iwasaki A and Yamanouchi K 2017 *Phys. Rev. A* **96** 041401
[98] Pavicić D, Lee K F, Rayner D M, Corkum P B and Villeneuve D M 2007 *Phys. Rev. Lett.* **98** 243001
[99] Li H L, Hou M Y, Zang H W, Fu Y, Lötstedt E, Ando T, Iwasaki A, Yamanouchi K and Xu H L 2019 *Phys. Rev. Lett.* **122** 013202
[100] Chang Z 2004 *Phys. Rev. A* **70** 043802
[101] Ni J, Chu W, Zhang H, Zeng B, Yao J, Qiao L, Li G, Jing C R, Xie H Q, Xu H, Cheng Y and Xu Z 2014 *Opt. Lett.* **39** 2250
[102] Froula D H, Turnbull D, Davies A S, Kessler T J, Haberberger D, Palastro J P, Bahk S W , Begishev I A, Boni R, Bucht S, Katz J and Shaw J L 2018 *Nat. Photon.* **12** 262